Inorganic Chemistry

Article

pubs.acs.org/IC

cRGD Peptide-Conjugated Icosahedral *closo*-B_{12}^{2-} Core Carrying Multiple Gd^{3+}-DOTA Chelates for $\alpha_v\beta_3$ Integrin-Targeted Tumor Imaging (MRI)

Lalit N. Goswami, Lixin Ma, Quanyu Cai, Saurav J. Sarma, Satish S. Jalisatgi, and M. Frederick Hawthorne*

International Institute of Nano and Molecular Medicine, School of Medicine, University of Missouri, Columbia, Missouri 65211-3450, United States

Supporting Information

ABSTRACT: A vertex-differentiated icosahedral *closo*-B_{12}^{2-} core was utilized to construct a $\alpha_v\beta_3$ integrin receptor-targeted (via cRGD peptide) high payload MRI contrast agent (**CA-12**) carrying 11 copies of Gd^{3+}-DOTA chelates attached to the *closo*-B_{12}^{2-} surface via suitable linkers. The resulting polyfunctional MRI contrast agent possessed a higher relaxivity value per-Gd compared to Omniscan, a small molecular contrast agent commonly used in clinical settings. The $\alpha_v\beta_3$ integrin receptor specificity of **CA-12** was confirmed via *in vitro* cellular binding experiments and *in vivo* MRI of mice bearing human PC-3 prostate cancer xenografts. Integrin $\alpha_v\beta_3$-positive MDA-MB-231 cells exhibited 300% higher uptake of **CA-12** than $\alpha_v\beta_3$-negative T47D cells. Serial T1-weighted MRI showed superior contrast enhancement of tumors by **CA-12** compared to both a nontargeted 12-fold Gd^{3+}-DOTA closomer control (**CA-7**) and Omniscan. Contrast enhancement by **CA-12** persisted for 4 h postinjection, and subsequent enhancement of kidney tissue indicated a renal elimination route similar to Omniscan. No toxic effects of **CA-12** were apparent in any mice for up to 24 h postinjection. Post-mortem ICP-OES analysis at 24 h detected no residual Gd in any of the tissue samples analyzed.

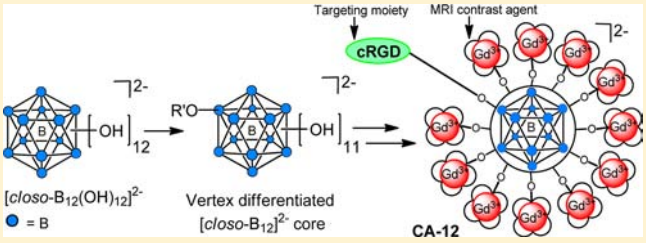

INTRODUCTION

Magnetic resonance imaging (MRI) is one of the most powerful diagnostic modalities in clinical medicine and biomedical research. The resolution and sensitivity of MRI is further enhanced through the administration of a contrast agent (CA). Due to their positive contrast enhancement properties, paramagnetic gadolinium-based small molecular CAs have been used most widely in clinical settings.[1] A significant drawback of these CAs is their lack of specificity and failure to provide sufficient contrast at low concentrations. With regard to cancer detection, targeting of MRI CA to cellular markers specifically expressed by tumor cells would greatly facilitate diagnosis, monitoring of disease progression, and assessment of treatment success. Research toward the development of targeted CAs has been ongoing, with most efforts directed toward conjugation of a CA to specific antibodies or a peptide.[2,3]

Efforts have also been directed at producing tissue specific MRI CAs.[4] In particular, the $\alpha_v\beta_3$ integrin receptor has been extensively investigated as a molecular target due to its involvement in angiogenesis, proliferation, and metastasis of several tumor types.[5] Integrin $\alpha_v\beta_3$ has high expression on proliferating endothelial cells during tumor angiogenesis and metastasis in contrast to resting cells.[6,7] Since the $\alpha_v\beta_3$ integrin receptors binds to certain extracellular matrix proteins via the peptide sequence Arg-Gly-Asp (RGD), diverse RGD peptide ligands have been investigated as a targeting agent for $\alpha_v\beta_3$ integrin.[8] In particular, the cyclic RGD peptide (cRGD) has a relatively high and specific affinity for $\alpha_v\beta_3$ integrin receptors. The synthesis of several small molecular MRI CAs possessing a cRGD peptide conjugated to a Gd^{3+}-chelate have been reported in the literature.[5]

However, small molecular CAs are in practice unsuitable for targeted imaging applications because of the high tissue concentrations of Gd^{3+} ions necessary to obtain sufficient contrast. Target receptors associated with particular tumor types or tissue pathologies are typically expressed at very low levels. In the case of $\alpha_v\beta_3$ integrin, the α_v and β_3 subunits number only 3×10^3 to 1.4×10^4 and 5.3×10^2 to 1.1×10^4 copies per cell, respectively.[9] In order to obtain sufficient contrast enhancement, the number of Gd^{3+} ions bound per target must be substantially increased.

The problem of insufficient Gd concentration in targeted imaging has been addressed by the use of macromolecules (dendrimers, liposomes, micelles, nanoparticles) to which large numbers of Gd^{3+}-chelates are attached along with targeting moieties.[10] Conjugation of Gd^{3+}-chelates to macromolecules offers the additional advantage of increasing the rotational correlation time, resulting in improved relaxivity (r_1) and therefore increased contrast enhancement.[11] However, despite

Received: October 25, 2012
Published: February 7, 2013

   dx.doi.org/10.1021/ic302340c | *Inorg. Chem.* 2013, 52, 1701−1709

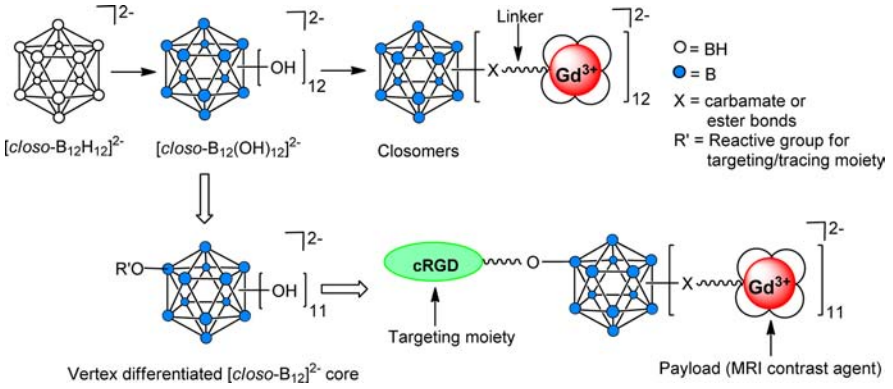

Figure 1. Schematic representation of a vertex-differentiated $[closo\text{-}B_{12}]^{2-}$ core supporting a targeting moiety (cRGD) and 11 copies of a MRI contrast agent.

Scheme 1. Synthesis of Amino-Terminated Hexaethylene Glycol (HEG) Linked DOTA Ligand 4[a]

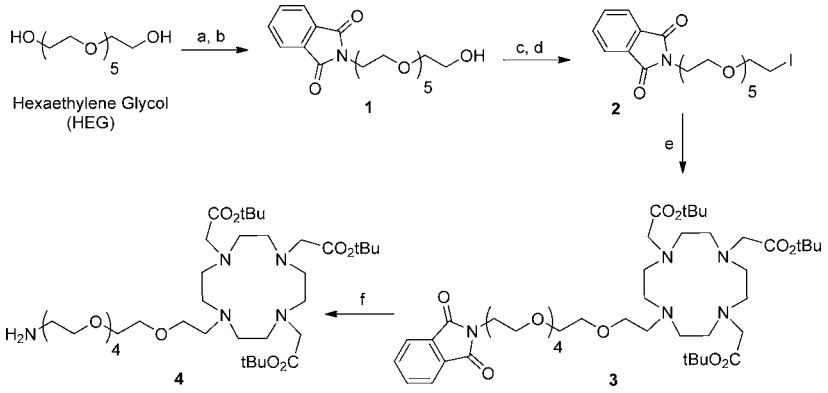

[a]Reagents and conditions: (a) 1.0 equiv methanesulfonyl chloride (MsCl), triethylamine (Et_3N), dichloromethane (DCM), 0 °C−RT, 3 h; (b) potassium phthalimide, *N*,*N*′-dimethylformamide (DMF), 110 °C, 15 h, 44% in two steps; (c) 1.3 equiv MsCl, Et_3N, DCM, 0 °C−RT, 3 h; (d) NaI, acetone, 65 °C, 15 h, 95% in two steps; (e) DO3A-*t*-Bu-ester, $KHCO_3$, DMF, 12 h, 60 °C, 96%; (f) hydrazine, ethanol, 65 °C, 3 h, 96%.

their satisfactory *in vivo* biodistribution profiles and high r_1 values, these macromolecular CAs suffer from the problem of polydispersity. Polydispersity has impact on the stability, solubility, appearance, and texture of the macromolecule and thus can affect the overall efficacy of the drug or imaging agent.

Polyhedral boranes and carboranes have generated considerable interest in biomedical research because of their potential as monodispersed nanocarriers of diagnostic and therapeutic agents.[12] Hydroxylation of all 12 B−H vertices[13] of icosahedral $[closo\text{-}B_{12}H_{12}]^{2-}$ to $[closo\text{-}B_{12}(OH)_{12}]^{2-}$ permits the attachment of up to 12 copies of a desired functionality through suitable linkers even at zero generation.[14] The 12 linker arms are in close proximity to one another, a configuration that makes these compounds ideally suited for the construction of monodispersed nanomolecular MRI CAs. In a companion paper, we reported the synthesis of the first such contrast agent, an icosahedral *closo*-B_{12}^{2} scaffold possessing 12 Gd^{3+}-chelates (Figure 1).[15]

Synthesis of a targeted nanomolecular CA requires the presence of heterobifunctionalized linker arms on the same scaffold to permit attachment of both the targeting moiety as well as multiple copies of Gd^{3+}-chelates. We recently developed a synthetic methodology to differentiate a single B−OH vertex of $[closo\text{-}B_{12}(OH)_{12}]^{2-}$ to provide $[closo\text{-}B_{12}(OR)(OH)_{11}]^{2-}$. This methodology permitted the preparation of several vertex-differentiated closomers $[closo\text{-}B_{12}(OR)(OR')_{11}]^{2-}$ utilizing orthogonal chemical reactions.[16]

As proof of principle, we herein report the first application of this unique approach to synthesize a tumor-targeting nanomolecular MRI CA derived from a vertex-differentiated icosahedral *closo*-B_{12}^{2-} core. This closomer supports an $\alpha_v\beta_3$ integrin-targeting peptide (cRGD) covalently linked to one vertex, with the remaining 11 vertices carrying a high payload of Gd^{3+}-chelates (Figure 1). Using a cell binding assay, we demonstrate the specificity of this targeted CA for $\alpha_v\beta_3$ integrin receptors. Also presented is a comparative analysis of the relaxivity and contrast enhancement kinetics of the targeted CA to a nontargeted 12-fold closomer CA and to the commercially available small molecular CA Omniscan.

RESULTS AND DISCUSSION

Synthesis of DOTA Ligands. For this study, 1,4,7,10-tetraazacyclododecane-1,4,7,10-tetraacetic acid (DOTA) was selected as the Gd^{3+}-chelating ligand because of the higher thermodynamic stability of Gd^{3+}-DOTA (log $K_{GdL} \sim 23$) relative to Gd^{3+}-DTPA (log $K_{GdL} \sim 22$; DTPA = diethylenetriaminepentaacetic acid) or Gd^{3+}-DTTA (log $K_{GdL} \sim 17-19$; DTTA = diethylenetriaminetetraacetic acid) chelates.[1c] An amino-terminated DOTA ligand (**4**) was prepared via a six-step synthesis starting from hexaethylene glycol (HEG) (**1**) (Scheme 1). First, a phthalimide-functionalized HEG linker (**1**) was synthesized from commercially available HEG via a two-step process that converted one of the two hydroxyl groups to a phthalimide group in 44% yield. The remaining hydroxyl

dx.doi.org/10.1021/ic302340c | *Inorg. Chem.* 2013, 52, 1701−1709

group in **1** was converted to a mesylate (−OMs) group, which upon reaction with sodium iodide gave iodo-terminated HEG linker **2** in quantitative yield. The reaction of **2** with DO3A-*t*-Bu-ester [where DO3A = 1,4,7,10-tetraazacyclododecane-1,4,7-tris(*t*-butyl acetate)] produced DOTA derivative **3** in 96% yield. Deprotection of the phthalimide group on **3** using hydrazine gave the desired amino-terminated HEG-linked DOTA derivative **4** in 96% yield. The structures of compounds **1**−**4** were characterized by IR, NMR, and HRMS spectroscopy.

Synthesis of 12-Fold Gd^{3+}-DOTA-Conjugated Closomer CA-7. The preparation of a closomer conjugated to 12 Gd^{3+}-DOTA chelates was accomplished in a stepwise procedure that relied upon our recently reported synthesis of 12-fold carbonate closomers capable of reacting with primary amines to yield 12-fold carbamate closomers.[14a] The carbonate closomer **5** was reacted with the amino-terminated DOTA ligand **4** to produce the 12-fold DOTA conjugate **6** in 80% yield (Scheme 2). Closomer **6** was purified by size-exclusion

Scheme 2. Synthesis of 12-Fold Gd^{3+}-DOTA Closomer Conjugate CA-7[a]

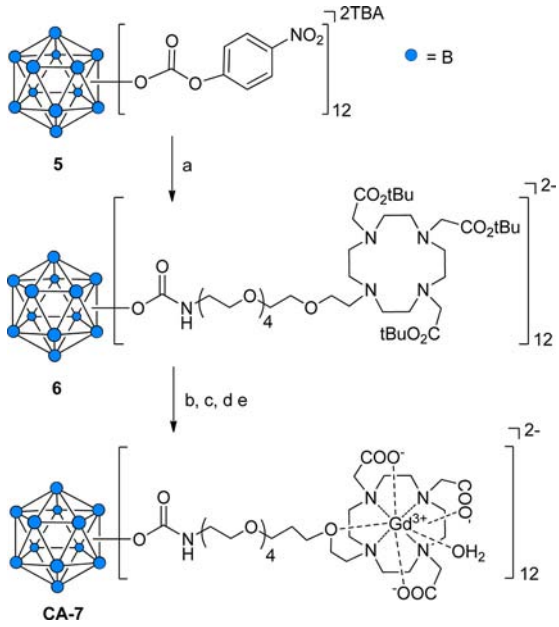

[a]Reagents and conditions: (a) **4**, acetonitrile (ACN), 7 days, RT, 80%; (b) 80% TFA-DCM, 6 h, RT; (c) $GdCl_3 \cdot 6H_2O$, citrate buffer, pH 7, 24 h, RT, sonication; (d) dialysis, 1000 molecular weight cutoff (MWCO), 48 h; (e) lyophilization, 71%.

column chromatography on Lipophilic Sephadex LH-20 using MeOH as the eluent and characterized by IR, NMR, and HRMS spectroscopy. To remove the *tert*-butyl ester groups present on the DOTA ligands, closomer **6** was treated with 80% trifluoroacetic acid (TFA) in DCM. Complete deprotection was confirmed by the absence of a large singlet at δ 1.47 ppm from the ^{1}H NMR spectrum of **6**. Gd^{3+} chelation was achieved by reacting deprotected closomer **6** with $GdCl_3 \cdot 6H_2O$ in citrate buffer at pH ∼ 7. Following extensive dialysis and lyophilization, the 12-fold Gd^{3+}-DOTA-conjugated closomer **CA-7** was obtained in 71% yield.

CA-7 was characterized by IR spectroscopy and inductively coupled plasma optical emission spectroscopy (ICP-OES) analysis. The IR spectrum of **CA-7** exhibited the characteristic shift of the carbonyl stretch from 1725 to 1605 cm^{-1} indicative of complexation of Gd^{3+} with the DOTA ligands (Supporting Information). The gadolinium/boron content of **CA-7** was determined using ICP-OES analysis. **CA-7** contained an average of 11.4 Gd^{3+} ions per closomer, indicating essentially fully loaded DOTA ligands. Mass spectrometry analysis of **CA-7** was unsuccessful; we could not obtain the desired mass peaks possibly due to the production of multiple charged species during the ionization step. The presence of free Gd^{3+} ions in the solution of closomer **CA-7** was determined by a spectrophotometric method using xylenol orange.[17] No free Gd^{3+} ions were detected. Dynamic light-scattering (DLS) analysis of **CA-7** in phosphate-buffered saline (PBS) and 2% Tween-80/PBS solution gave an average particle size of 10 nm (Supporting Information).

Synthesis of Targeted 11-Fold Gd^{3+}-DOTA Conjugated Closomer CA-12. The synthesis of a targeted MRI CA assembled on an icosahedral *closo*-B_{12}^{2-} core is based on our recently published work regarding preparation of vertex-differentiated closomers.[16] Attachment of the targeting peptide cRGD was accomplished by an azide−alkyne click reaction of alkyne-terminated cRGD peptide derivative **8**[18] with the 11-fold carbonate closomer **9**,[16] which possesses an azido-termined linker at a single vertex (Scheme 3). The resulting cRGD-conjugated closomer **10** was purified by size-exclusion column chromatography on Lipophilic Sephadex LH-20 using MeOH as the eluent. Purified closomer **10** was characterized by NMR and HRMS spectroscopy. The ^{1}H NMR spectral analysis of **10** showed a singlet at δ 7.94 ppm attributed to the single proton of the 1,4-triazole group, confirming attachment of the cRGD peptide.

Addition of DOTA ligands to the remaining 11 vertices of cRGD-conjugated closomer **10** was accomplished by reaction with amino-terminated DOTA derivative **4** (5 equiv per vertex) in ACN for seven days at RT to obtain the 11-fold carbamate closomer **11** in 83% yield (Scheme 3). Closomer **11** was purified by size-exclusion column chromatography on Lipophilic Sephadex LH-20 using MeOH as the eluent and its structure was verified by IR, NMR, and HRMS spectroscopy. Removal of the *tert*-butyl ester groups from **11** was achieved by treatment with 80% TFA in DCM. Complete deprotection of *tert*-butyl ester groups from **11** was confirmed by the absence of the large singlet at δ 1.50 ppm from its ^{1}H NMR spectrum.

Deprotected closomer **11** was reacted with $GdCl_3 \cdot 6H_2O$ (10 equiv per vertex) in citrate buffer at pH ∼ 7 to give closomer **CA-12** in 69% yield. **CA-12** was purified by exhaustive dialysis in ultrapure water and was characterized by IR spectroscopy and ICP-OES analysis. IR spectral analysis showed a characteristic shift of the carbonyl stretch from 1730 to 1595 cm^{-1}, confirming complexation of Gd^{3+} with the DOTA ligands. The mass spectrometry analysis of **CA-12** was unsuccessful; however, the ICP-OES analysis of **CA-12** showed an average of 10.6 Gd^{3+} ions per closomer, indicating the formation of essentially fully loaded complex. The presence of any free Gd^{3+} ions in solution of targeted closomer **CA-12** was determined by a spectrophotometric method using xylenol orange.[17] No free Gd^{3+} ions were detected in the solution. DLS analysis of **CA-12** in PBS and 2% Tween-80/PBS solution gave an average particle size of 12−13 nm (Supporting Information).

Relaxivity Studies. The per-Gd relaxivity (r_1) of **CA-7**, **CA-12**, and Omniscan at 25 °C and 7 T were compared in three different formulations: PBS, 2% Tween/PBS, and bovine calf serum (Figure 2). The relaxivity of each contrast agent was relatively unaffected by formulation type, but the r_1 values of

dx.doi.org/10.1021/ic302340c | Inorg. Chem. 2013, 52, 1701−1709

Scheme 3. Synthesis of 11-Fold Gd^{+3}-DOTA-cRGD Closomer Conjugate CA-12[a]

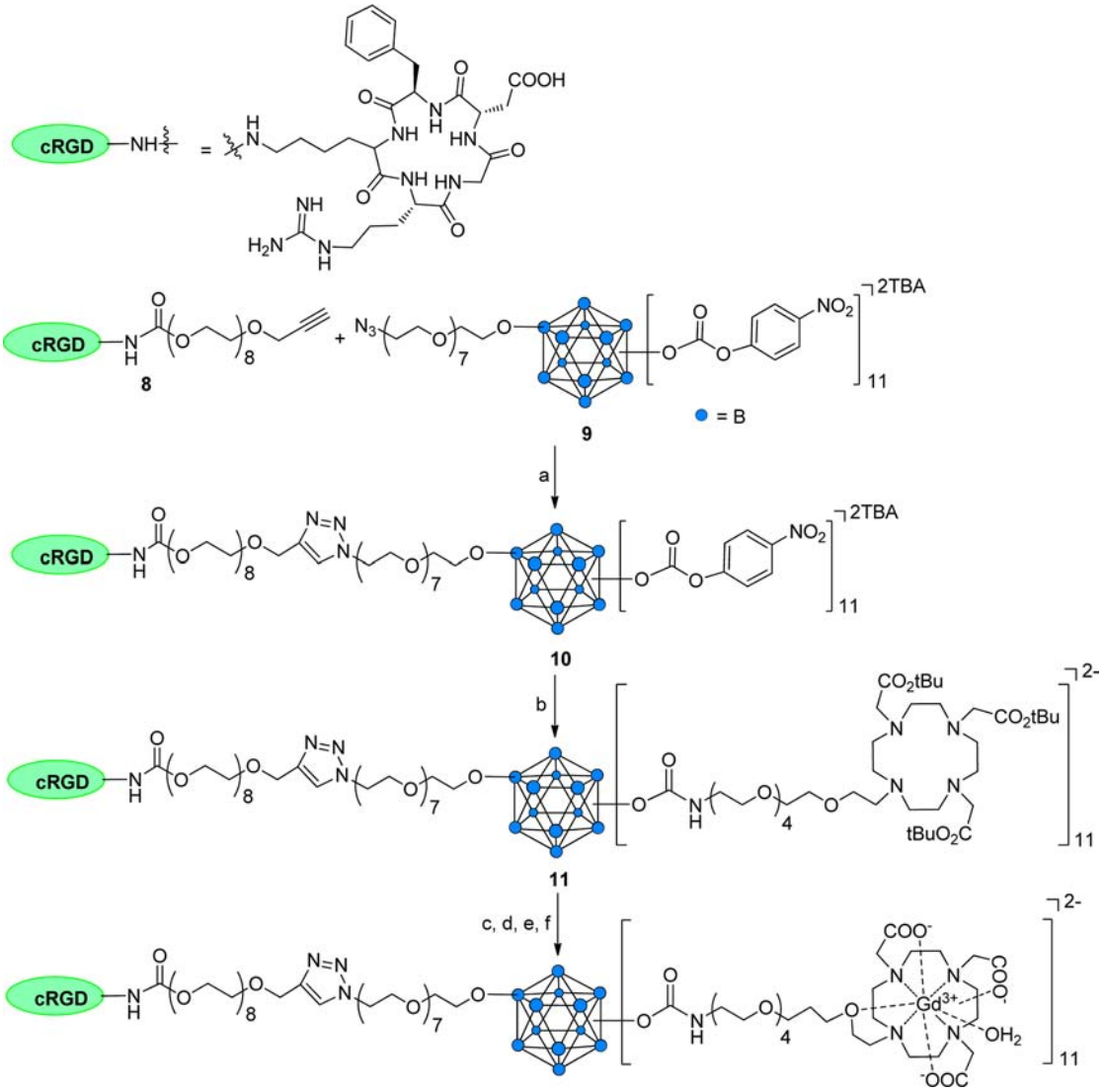

[a]Reagents and conditions: (a) CuI, *N*,*N*-diisopropylethylamine (DIPEA), THF-ACN, 15 h, RT, 87%; (b) **4**, ACN, 7 days, RT, 83%; (c) 80% TFA-DCM, 6 h, RT; (d) $GdCl_3 \cdot 6H_2O$, citrate buffer, pH 7, 24 h, RT, sonication; (e) dialysis, 1000 MWCO, 48 h; (f) lyophilization, 69%.

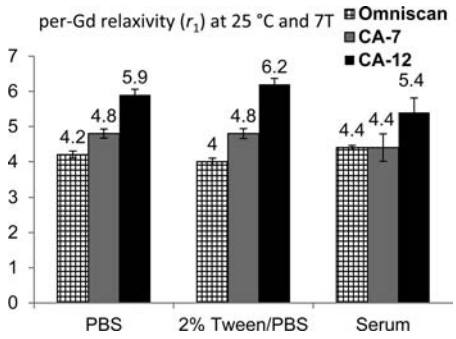

Figure 2. Relaxivity (r_1) profile of **CA-7**, **CA-12**, and Omniscan in three different formulations at 25 °C and 7 T.

CA-7 and **CA-12** were slightly higher than Omniscan (4.2 mM^{-1} s^{-1} in PBS) across all formulations. Nonetheless, the r_1 values for **CA-7** and **CA-12** (e.g., 4.8 mM^{-1} s^{-1} per Gd and 5.9 mM^{-1} s^{-1} per Gd in PBS) fall well within the range of other macromolecular MRI CAs carrying multiple Gd^{3+} chelates that have one inner sphere water-exchange site.[11] Macromolecular CAs are known to exhibit higher r_1 values due to their larger size and the confinement of the Gd^{3+} ions in a sterically constrained space. However, the slightly higher r_1 values of **CA-12** compared to **CA-7** may result from slower rotation (τ_R) of the Gd^{3+} chelates due to the attachment of the cRGD peptide to the icosahedral *closo*-B_{12}^{2-} core.

Molecular relaxivity values for **CA-7** and **CA-12** were calculated on the basis of the number of Gd^{3+} ions per closomer. **CA-7** and **CA-12** have an average 11.4 and 10.6 Gd^{3+} ions per closomer, respectively, giving molecular relaxivity values of 54.7 and 62.5 mM^{-1} s^{-1} per closomer. The T1-weighted MRI images of **CA-12**, **CA-7**, and Omniscan at 7 T presented in Figure 3 show greater contrast enhancement for **CA-12** and **CA-7** compared to Omniscan due to their higher relaxivity values.

Cell Binding Studies. To establish the specificity of cRGD-closomer conjugate **CA-12** for $\alpha_v\beta_3$ integrin receptors, *in vitro* binding experiments were performed using MDA-MB-231 and T47D cells. MDA-MB-231 cells express high levels of $\alpha_v\beta_3$

dx.doi.org/10.1021/ic302340c | *Inorg. Chem.* 2013, 52, 1701−1709

Figure 3. T1-weighted MRI images of **CA-12**, **CA-7**, and Omniscan at 1 mM Gd concentration in PBS (25 °C and 7 T).

integrins ($\alpha_v\beta_3$ positive), whereas T47D cells lack $\alpha_v\beta_3$ integrin receptors ($\alpha_v\beta_3$ negative).[19] Cells were incubated with **CA-12** for 30 min at 37 °C (Gd concentration 5 mM, PBS), and the gadolinium concentration in lysed cell pellets was measured using ICP-OES analysis. The Gd concentration was 300% higher in MDA-MB-231 cells relative to T47D cells (Figure 4), demonstrating the ability of cRGD-containing closomer conjugate **CA-12** to target cells expressing $\alpha_v\beta_3$ integrin receptors.

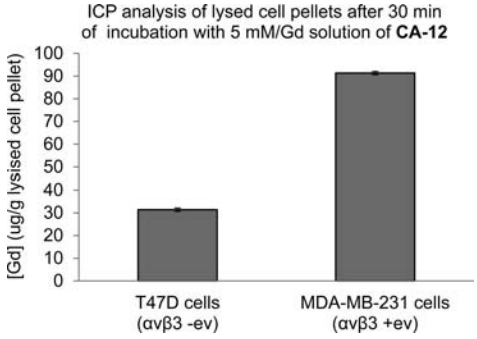

Figure 4. Gadolinium concentration in lysed pellets of cells incubated with **CA-12** (5 mM Gd, PBS) determined by ICP-OES.

***In Vivo* MRI studies.** The ability of **CA-12** to specifically target $\alpha_v\beta_3$ integrin-expressing tumors *in vivo* was also investigated by MRI of severely compromised immunodeficient (SCID) mice bearing human PC-3 prostate cancer xenografts. There were 18 mice subjected to MRI scanning following intravenous injection of either cRDG-containing **CA-12**, nontargeted closomer **CA-7**, or Omniscan at a gadolinium dose of 0.04 mmol/kg body weight. Six mice were included in each of the three experimental groups.

T1-weighted MRI scans showed that tumors of mice injected with targeted closomer **CA-12** exhibited strong contrast enhancement for up to 4 h postinjection (Figure 5A). Significant contrast enhancement by **CA-7** persisted for only 1 h postinjection (Figure 5B). Contrast enhancement by Omniscan diminished within 30 min postinjection, and no enhancement was detectable by 4 h postinjection (Figure 5C). MRI imaging also showed that contrast enhancement of the kidneys was higher and lasted longer in mice injected with **CA-12** (Figure 5A) compared to those injected with **CA-7** or Omniscan (Figure 5B,C), indicative of the relatively slower renal clearance of **CA-12**.

Calculation of the contrast enhancement ratios (CERs) for tumor and kidney tissues permitted a quantitative assessment of the relative enhancement capacity of **CA-12**, the nontargeted closomer **CA-7**, and Omniscan. In tumor tissue, the CER did not decline significantly until 24 h postinjection of **CA-12**, whereas it declined substantially by 4 and 1 h postinjection of **CA-7** and Omniscan, respectively (Figure 6). At 1 and 4 h postinjection of **CA-12**, tumor tissues had significantly higher CERs compared to those with **CA-7** ($P < 0.01$ at 1 h) and Omniscan ($P < 0.01$ at 1 h; $P < 0.05$ at 4 h). Similarly, the CER

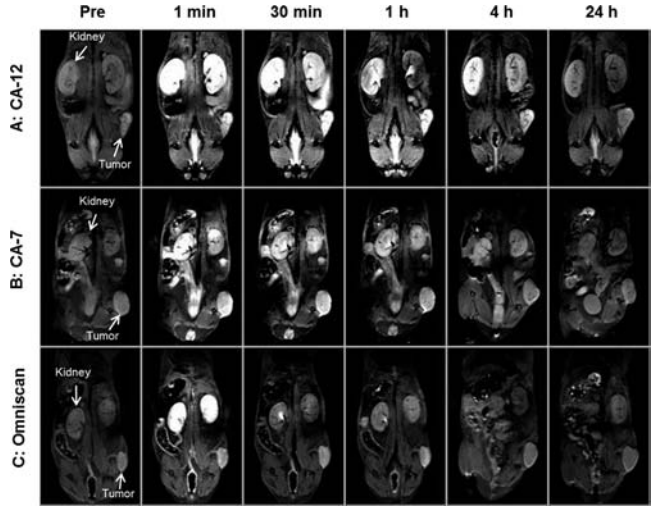

Figure 5. Representative *in vivo* T1-weighted MRI scans of mice ($n = 6$ mice for each experimental group) preinjection and at 1 min, 30 min, 1 h, 4 h, and 24 h postinjection of (A) **CA-12**, (B) **CA-7**, and (C) Omniscan (gadolinium dose of 0.04 mmol/kg).

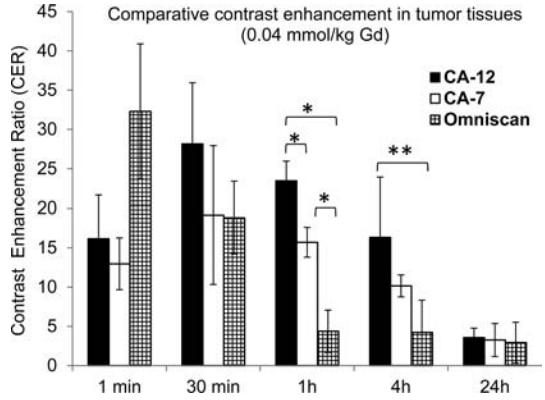

Figure 6. Contrast enhancement ratios (CERs) for tumor tissues of mice as a function of time measured from the *in vivo* imaging experiments after intravenous injection of **CA-12**, **CA-7**, or Omniscan with a gadolinium dose of 0.04 mmol/kg. *$P < 0.01$, **$P < 0.05$.

values for kidneys of mice injected with **CA-12** and **CA-7** initially increased and then declined, though at a slower rate than for kidneys of mice injected with Omniscan (Figure 7). For example, the kidney signals are higher at 1 h postinjection of **CA-12** compared to Omniscan ($P < 0.01$), and diminished to the baseline contrast at 24 h. The persistence of contrast in tumors and the slower renal clearance of **CA-12** may be attributed to the specific binding to integrin receptors by the cRGD ligand.

After 24 h, all mice were euthanized, and tail, blood, heart, lungs, liver, spleen, stomach, large and small intestines, kidneys, brain, and muscle tissues were analyzed for the presence of gadolinium ions using ICP-OES. No gadolinium was detectable in any of the tissues, indicating complete elimination of the CAs.

■ CONCLUSIONS

We have shown for the first time the utility of a vertex-differentiated icosahedral *closo*-B_{12}^{2-} core in the synthesis of a novel $\alpha_v\beta_3$ integrin-targeted polyfunctional MRI CA. The closomer **CA-12** carries a single cRGD peptide attached to the

dx.doi.org/10.1021/ic302340c | *Inorg. Chem.* 2013, 52, 1701−1709

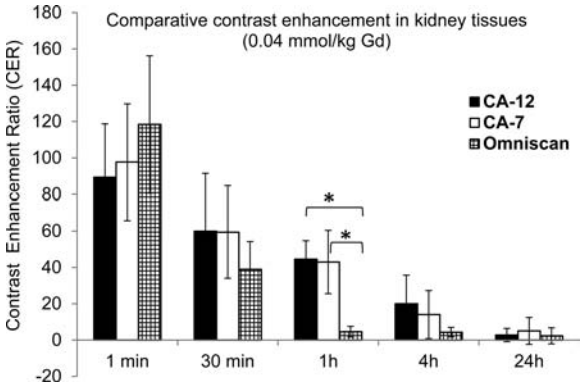

Figure 7. Contrast enhancement ratios (or CERs) for kidney tissues of mice as a function of time measured from the *in vivo* imaging experiments after intravenous injection of **CA-12**, **CA-7**, or Omniscan with a gadolinium dose of 0.04 mmol/kg. *$P < 0.01$.

closo-B_{12}^{2-} core via a long PEG linker and holds 11 Gd^{3+}-DOTA chelates attached through a HEG linker via carbamate linkages. This unique MRI CA exhibits a higher relaxivity per Gd than the small molecular CA Omniscan in PBS at 7 T.

In vitro cell binding experiments and *in vivo* MRI analysis of tumor-bearing mice demonstrated the ability of **CA-12** to selectively target integrin $\alpha_v\beta_3$-expressing cells. Binding studies showed that the Gd content was 3-fold higher in cells expressing $\alpha_v\beta_3$ receptors compared to cells in which receptor expression was absent. Serial T1-weighted MRI of mice possessing human PC-3 prostate cancer xenographs showed that higher and more persistent contrast enhancement of tumors was achieved with **CA-12** than with Omniscan or with **CA-7**, a closomer carrying 12 Gd^{3+}-DOTA chelates but lacking the cRGD peptide. Mice exhibited no apparent toxic effects from any of the CA for 24 h postinjection, and post-mortem ICP-OES analysis of numerous tissues found no detectable residual Gd.

The methodology presented here is versatile and should be highly useful in the development of a wide variety of high-payload, receptor-specific diagnostic and therapeutic agents. We are currently pursuing work in this direction.

EXPERIMENTAL SECTION

General Information. Common reagents and chromatographic solvents were obtained from commercial suppliers (Sigma-Aldrich, Fisher Scientific, and Acros Organics) and used without any further purification. Lipophilic Sephadex LH-20 was obtained from GE Healthcare. DO3A-*t*-Bu-ester and cRGD peptide were purchased from Macrocyclics, Inc., and Peptides International, respectively. NMR spectra were recorded on Bruker Avance 400 and 500 MHz spectrometers. The high-resolution mass spectrometry analysis was performed using Applied Biosystems Mariner ESI-TOF. IR spectra were recorded on Thermo Nicolet FT-IR spectrometer. The dynamic light scattering analysis was performed on a Microtrac Zetatrac particle size analyzer. Gadolinium (Gd^{3+}) concentrations of the samples were measured by inductively coupled plasma optical emission spectroscopy (ICP-OES) on a PerkinElmer OptimaTM 7000 DV instrument. All the Gd^{3+} and boron concentrations obtained via ICP analysis are the average of three measurements. The error bars provided in the figures are standard deviations.

Synthesis of 1. To a mixture of Et_3N (2.70 g, 26.6 mmol) and hexaethylene glycol (5.00 g, 17.7 mmol) in DCM (50 mL) stirring at 0 °C was added a solution of MsCl (2.03 g, 17.7 mmol) in DCM (20 mL) over 1 h period by syringe pump. After addition of MsCl, the reaction was allowed to proceed at 0 °C for 1 h, and then at RT for 2 h. The reaction mixture was concentrated to dryness. The residue was dissolved in DCM (100 mL) and washed with 3% HCl−water (100 mL) and brine (100 mL). The organic layer was separated, dried over Na_2SO_4, and then concentrated and dried under high vacuum. The dried sample was dissolved in DMF (30 mL) to which potassium phthalimide (4.26 g, 23.0 mmol) was added, and the mixture was stirred at 110 °C for 15 h. Following concentration under high vacuum to remove the DMF, the resulting solid was dissolved in Et_2O and filtered through a Celite pad. The filtrate was concentrated, and the crude material was purified on a silica gel column to obtain pure product as a colorless oil. Yield: 3.2 g (44%). ^{1}H NMR (400 MHz, $CDCl_3$): δ 7.70 (dd, 2H, J = 2.8 and 5.2 Hz, −*CH*−Pth), 7.59 (dd, 2H, J = 2.8 and 5.2 Hz, −*CH*−Pth), 4.28 (br s, 1H, −OH), 3.77 (t, 2H, J = 5.6 Hz, −OCH_2HEG), 3.60 (m, 4H, −OCH_2HEG), 3.52−3.45 (m, 18H, −OCH_2HEG). ^{13}C NMR (100.6 MHz, $CDCl_3$): δ 167.50, 161.98, 133.43, 133.03, 131.45, 122.53, 122.21, 72.03, 69.98−69.44 (multiple peaks), 67.21, 60.79, 36.68, 35.83, 30.73. HRMS (ESI): m/z calcd for $C_{20}H_{29}NO_8$ $[M + Na]^+$ 434.1785; found 434.1575. For $C_{20}H_{29}NO_8$ $[M + K]^+$ 450.1525; found 450.1038.

Synthesis of 2. To a mixture of Et_3N (1.10 g, 10.9 mmol) and **1** (3.00 g, 7.29 mmol) in DCM (30 mL) stirring at 0 °C was added a solution of MsCl (1.08 g, 9.48 mmol) in DCM (10 mL) over 1 h by syringe pump. After addition, the reaction was allowed to proceed at 0 °C for 1 h and then at room temperature for 2 h. The reaction mixture was concentrated to dryness, and the residue was then dissolved in DCM (100 mL). After successive washing with 3% HCl−water (100 mL) and brine (100 mL), the organic layer was separated, dried over Na_2SO_4, and then concentrated and dried under high vacuum. The dried sample was then dissolved in acetone, sodium iodide (4.37 g, 29.1 mmol) was added to it, and the resulting mixture was stirred at 65 °C for 15 h. The reaction mixture was then concentrated to dryness, DCM (100 mL) was added, and the solution was filtered through a Celite pad. The filtrate was concentrated and purified by silica gel chromatography to obtain pure product as a colorless oil. Yield: 3.6 g (95%). ^{1}H NMR (400 MHz, $CDCl_3$): δ 7.76 (dd, 2H, J = 3.2 and 5.6 Hz, −*CH*−Pth), 7.65 (dd, 2H, J = 2.8 and 5.2 Hz, −*CH*−Pth), 3.81 (t, 2H, J = 6.0 Hz, −OCH_2HEG), 3.67 (m, 4H, −OCH_2HEG), 3.59−3.50 (m, 16H, −OCH_2HEG), 3.18 (t, 2H, J = 7.2 Hz, −OCH_2HEG). ^{13}C NMR (100.6 MHz, $CDCl_3$): δ 167.96, 133.77, 131.93, 123.02, 71.75, 70.45−69.92 (multiple peaks), 67.70, 37.10, 2.98. HRMS (ESI): m/z calcd for $C_{20}H_{28}INO_7$ $[M + Na]^+$ 544.0803; found 544.0283.

Synthesis of 3. To a mixture of DO3A-*t*-Bu-ester (2.00 g, 3.88 mmol) and **2** (3.04 g, 5.83 mmol) in DMF (25 mL) was added $KHCO_3$ (0.78 g, 7.77 mmol), and the mixture was stirred at 60 °C for 15 h. The reaction mixture was cooled and DCM (100 mL) added. The mixture was washed with brine (100 mL), and the organic layer was separated, dried over Na_2SO_4, and concentrated. After column chromatography over alumina(IV), the pure product was obtained as a viscous oil. Yield: 3.4 g (96%). ^{1}H NMR (400 MHz, $CDCl_3$): δ 7.63−7.60 (m, 4H, −*CH*−Pth), 3.68 (t, 2H, J = 5.6 Hz, −OCH_2HEG), 3.55 (t, 2H, J = 5.6 Hz, −OCH_2HEG), 3.45−3.36 (m, 18H, −OCH_2HEG), 3.10−2.00 (m, 24H, −OCH_2HEG and −CH_2DOTA), 1.28 (m, 27H, −^{t}*But*−DOTA). ^{13}C NMR (100.6 MHz, $CDCl_3$): δ 171.95, 167.61, 133.69, 131.41, 122.60, 81.63, 69.69−69.12 (multiple peaks), 67.24, 66.57, 55.81, 55.06, 53.37, 51.60, 49.49, 49.17, 36.65, 27.48. HRMS (ESI): m/z calcd for $C_{46}H_{77}N_5O_{13}$ $[M+Na]^+$ 930.5410; found 930.5362.

Synthesis of 4. A mixture of **3** (4.4 g, 4.84 mmol) and hydrazine (1.55 g, 48.4 mmol) in EtOH (60 mL) was stirred at 65 °C for 3 h. Upon reaction completion, the reaction mixture was concentrated to dryness. The residue was dissolved in DCM (100 mL) and filtered using a sintered glass funnel. The filtrate was concentrated and dried under high vacuum. Following column chromatography of the crude product over alumina(IV), pure product was obtained as a viscous oil. Yield: 3.6 g (96%). ^{1}H NMR (400 MHz, $CDCl_3$): δ 3.24−3.16 (m, 20H), 2.88 (m, 2H), 2.78−2.59 (m, 4H), 2.56−1.83 (m, 20H), 1.07 (m, 27H, −^{t}*But*−DOTA). ^{13}C NMR (100.6 MHz, $CDCl_3$): δ 171.68, 171.40, 81.01, 80.98, 71.35, 69.35−69.04 (multiple peaks), 68.74, 68.55, 66.10, 55.28, 54.53, 53.11, 51.10, 49.47, 48.67, 40.35, 27.09, 26.83. HRMS (ESI): m/z calcd for $C_{38}H_{75}N_5O_{11}$ $[M+Na]^+$ 800.5355; found 800.5723.

dx.doi.org/10.1021/ic302340c | *Inorg. Chem.* 2013, 52, 1701−1709

Synthesis of Closomer 6. A mixture of 12-fold 4-nitrophenyl carbonate closomer **5** (0.20 g, 0.07 mmol) and DOTA ligand **4** (3.33 g, 4.28 mmol) in ACN (30 mL) was stirred for 7 days at RT under an argon atmosphere. The reaction mixture was then concentrated and purified via size-exclusion chromatography over Lipophilic Sephadex LH-20 using MeOH as the eluent. The product was obtained as a sticky, light-brown solid. Mp: 65−68 °C. Yield: 0.60 g (80%). ^{1}H NMR (400 MHz, CD_3CN): δ 6.57 (br s, 10H), 3.79−2.13 (m, 554H), 1.47 (m, 324H). ^{13}C NMR (100.6 MHz, CD_3CN): δ 173.8, 173.66, 171.50, 171.25, 82.74, 81.75, 71.02−70.35 (multiple peaks), 68.1, 57.19, 56.97, 56.31, 55.92, 55.28, 53.62, 53.17, 51.15, 50.66, 41.80, 28.34, 28.26, 28.14. ^{11}B NMR (160.4 MHz, CD_3CN): δ −18.19. HRMS (m/z): av mass calcd for $C_{468}H_{888}B_{12}N_{60}O_{156}$ $[M + 6H]^{4+}$ + 2K + Na + TBA 2838.7986 (TBA = tetrabutyl ammonium); found 2838.5745. Calcd for $C_{468}H_{888}B_{12}N_{60}O_{156}$ $[M + 6H]^{4+}$ + 2K + 2Na + TBA 2861.7986; found 2861.6614.

Synthesis of 12-Fold DOTA-Gd Closomer CA-7. Closomer **6** (0.33 g, 0.03 mmol) was treated with 80% TFA/DCM (10 mL) for 6 h at RT under an argon atmosphere. The reaction mixture was then concentrated under reduced pressure. The resulting residue was dissolved in a minimum amount of methanol, and the product was precipitated by adding ether. The solid product was filtered, washed with ether, and dried under high vacuum overnight. The now deprotected closomer **6** was dissolved in 1 M citrate buffer (15 mL, pH 7) and added to a solution of $GdCl_3.6H_2O$ (1.40 g, 3.78 mmol, in 15 mL of 1 M citrate buffer, pH 7) over 5 h at RT with vigorous stirring. The reaction mixture was maintained at approximately pH 7 using 0.3 N NaOH. When addition of **6** was complete, the reaction mixture was stirred for an additional 24 h at RT. To avoid possible aggregation and intermolecular chelation of Gd^{3+}, the reaction mixture was sonicated a few times over the entire course of the reaction. To remove excess $GdCl_3$, the reaction mixture was dialyzed in deionized water for 48 h using 1000 MWCO dialysis tubing (Spectra/Por). Following lyophilization, the product **CA-7** was obtained as an off-white solid. Mp: 255−260 °C (decomposed). Yield: 0.22 g (71%). ICP-OES analysis: calcd av Gd per closomer 12; found 11.4. The mass spectrometry analysis attempts were unsuccessful.

Synthesis of Alkyne-Terminated cRGD Conjugate 8. Alkyne-terminated cRGD conjugate **8** was synthesized according to our recently published procedure.[19]

Synthesis of 11-Fold 4-Nitrophenyl Carbonate Closomer 9. Closomer **9** was synthesized according to our recently described method.[16]

Synthesis of Closomer 10. 11-Fold 4-nitrophenyl carbonate closomer **9** (0.03 g, 9.90×10^{-3} mmol), alkyne-terminated cRGD conjugate **8** (10.3 mg, 9.90×10^{-3} mmol), and copper(I) iodide (2.80 mg, 14.7×10^{-3} mmol) were dissolved in a 1:1 mixture of THF and ACN (6 mL). After addition of DIPEA (20 mg, excess), the reaction mixture was vigorously stirred at RT for 15 h under an argon atmosphere. Upon reaction completion, the reaction mixture was concentrated to remove THF and ACN. The residue was dissolved in ethyl acetate and filtered through a Celite pad. The filtrate was concentrated, and the crude product was purified via size-exclusion column chromatography on Lipophilic Sephadex LH-20 using ACN as the eluent. The purified product was obtained as a sticky, light-yellow solid. Yield: 35.0 mg (87%). ^{1}H NMR (500 MHz, CD_3CN): δ 8.72 (m, 22H), 7.94 (s, 1H), 7.39 (m, 24H), 7.13 (m, 2H), 6.90 (m, 1H), 4.65−4.58 (m, 4H), 4.21 (s, 2H), 3.99−3.91 (m, 6H), 3.62 (m, 76H), 3.16 (m, 13H), 2.30 (m, 6H), 2.06 (m, 8H), 1.94 (m, 2H), 1.68 (m, 10H), 1.44−1.31 (m, 15H), 1.16 (m, 2H), 1.05 (m, 14H) (fewer proton counts for TBA^+ is due to exchange with H_3O^+ and Na^+). ^{13}C NMR (125.7 MHz, CD_3CN): δ 156.63, 150.96, 150.69, 145.12, 127.63, 125.09, 122.31, 70.13−68.93 (multiple peaks), 63.78, 58.33, 46.93, 23.30, 19.33, 12.80, 8.23. ^{11}B NMR (160.4 MHz, CD_3CN): δ −14.34, −18.12. HRMS (m/z): av mass calcd for $C_{140}H_{150}B_{12}N_{22}O_{81}$ $[M]^{2-}$ 1783.4705; found 1783.4463.

Synthesis of Closomer 11. A mixture of closomer **10** (0.03 g, 7.40×10^{-3} mmol) and DOTA ligand **4** (0.32 g, 0.40 mmol) in ACN (10 mL) was stirred for 7 days at RT under an argon atmosphere. The reaction mixture was concentrated and purified via size-exclusion chromatography over Lipophilic Sephadex LH-20 using MeOH as the eluent. The pure product was obtained as a sticky, light-brown solid. Mp: 72−75 °C. Yield: 65.0 mg (83%). ^{1}H NMR (400 MHz, CD_3OD): δ 8.09 (s, 1H), 7.30−7.16 (m, 5H), 7.05 (m, 2H), 6.80 (m, 2H), 6.70 (m, 1H), 4.66 (m, 7H), 4.52−2.35 (m, 590H), 1.54−1.51 (m, 300H), 1.16 (m, 6H), 0.95 (m, 6H). ^{13}C NMR (100.6 MHz, CD_3CN): δ 173.78, 173.66, 171.25, 156.05, 130.28, 128.82, 124.9, 82.74, 82.72, 81.85, 71.02−69.87 (multiple peaks), 68.20, 57.19 (multiple peaks), 56.31, 55.71, 55.15, 53.55−53.23 (multiple peaks), 50.66 (multiple peaks), 48.43, 41.80, 28.26 (multiple peaks). ^{11}B NMR (160.4 MHz, CD_3CN): δ −14.54, −18.32. HRMS (m/z): av mass calcd for $C_{492}H_{920}B_{12}N_{66}O_{169}$ $[M + 6H]^{4+}$ + Na 2671.647030; found 2670.9688.

Synthesis of cRGD Conjugated 11-Fold DOTA-Gd Closomer CA-12. Closomer **11** (0.09 g, 8.40×10^{-3} mmol) was treated with 80% TFA/DCM (10 mL) for 6 h at RT under an argon atmosphere. The reaction mixture was concentrated under reduced pressure, and the residue was dissolved in a minimum amount of methanol. Ether was added to precipitate the solid product. The product was filtered, washed with additional ether, and dried under high vacuum overnight. The now-deprotected closomer **11** was dissolved in 1 M citrate buffer (15 mL, pH 7) and added to a solution of $GdCl_3.6H_2O$ (0.34 g, 0.92 mmol, in 15 mL of 1 M citrate buffer, pH 7) over 5 h at RT with vigorous stirring. The reaction mixture was maintained at approximately pH 7 using 0.3 N NaOH. When addition of **11** was complete, the reaction mixture was stirred at RT for an additional 24 h. To avoid possible aggregation and intermolecular chelation, the reaction mixture was sonicated a few times over the entire course of the reaction. The reaction mixture was then dialyzed in deionized water for 48 h using 1000 MWCO dialysis tubing (Spectra/Por). Following lyophilization, the product **CA-12** was obtained as an off-white solid. Mp: 207−210 °C (decomposed). Yield: 63.0 mg (69%). ICP-OES analysis: calcd av Gd per closomer 11; found: 10.6. Attempts at mass spectrometry analysis were unsuccessful.

Relaxivity Determinations. Solutions of **CA-7** and **CA-12** and Omniscan were prepared in PBS, 2% Tween-80/PBS, and bovine calf serum. T1 relaxation rates were determined for each of the three formulations of **CA-12** and **CA-7** at Gd^{3+} ion concentrations of 0.25, 0.5, and 1 mM. The Gd^{3+} ion concentration of Omniscan was 1 mM. The measurements were repeated on two or more independently prepared samples to ensure consistency. A buffer matched blank sample (0 mM) was also used in the relaxivity measurements of each sample.

Measurements were performed using a 7 T Varian Unity Inova MRI system (Varian Inc./Agilent Technologies) at RT. A T1-weighted MRI pulse sequence was applied with TE = 15 ms, and TR = 500 ms, slice thickness = 1 mm, matrix = 256 × 256, and FOV = 30 × 30 mm. A series of inversion recovery (IR) spin−echo images were acquired using TR = 3 s, TE = 15 ms, and the following inversion delays: 0.082, 0.1, 0.12, 0.16, 0.24, 0.32, 0.64, 1.28, 2.56, 3.6 s. Water signal intensities were measured using VnmrJ2.1D software (Varian Inc. /Agilent Technologies, 2005). Relaxation rates were calculated using a three-parameter experiential recovery fitting in Origin 8.5.0 (OriginLab Corporation, 2012).

Cell Binding Assays. MDA-MB-231 and T47D cells were obtained from the American Type Culture Collection (Manassas, VA). Cell culture reagents were purchased from Fisher Scientific (Chicago, IL) or Sigma-Aldrich (St. Louis, MO). Cells were cultured in complete growth medium [DMEM/F12 containing 10% heat-inactivated fetal bovine serum (FBS; Hyclone Laboratories, Logan, UT), 1% antibiotics] in a humidified incubator at 37 °C and 5% CO_2. When cells had reached approximately 70% confluency (3 days), they were treated with trypsin-EDTA solution and washed twice with cold PBS. The cells were counted using a hemacytometer and diluted with PBS to a concentration of 1×10^7 cell/mL. Cells were incubated with **CA-12** (Gd concentration 5 mM) in a 37 °C water bath for 30 min. After incubation, cells were centrifuged at 800 × g at 4 °C for 4 min, and the supernatant was removed. The pellet was washed twice with PBS, and cells were resuspended in 200 μL PBS. ICP-OES was used to measure the gadolinium concentration of the cells.

dx.doi.org/10.1021/ic302340c | Inorg. Chem. 2013, 52, 1701−1709

***In Vivo* MRI Analysis.** *In vivo* MRI studies were performed in severely compromised immunodeficient (SCID) mice bearing human PC-3 prostate cancer xenografts. Animal studies were conducted in accordance with the highest standards of care as outlined in the NIH's guide for care and use of laboratory animals and in accordance with policy and procedures for animal research at the Harry S. Truman Memorial Veterans Hospital. Four-to-five-week-old SCID mice were obtained from Taconic (Germantown, NY). Mice were housed four animals per cage in sterile microisolator cages in a temperature- and humidity-controlled room with a 12-h light/dark schedule. The animals were fed autoclaved rodent chow (Ralston Purina Company, St. Louis, MO) and provided water *ad libitum*. Mice were inoculated with human prostate cancer PC-3 tumor cells on the right flank. There were 18 mice, 6 mice in each experimental group, used in MRI experiments between 3 and 4 weeks post inoculation of tumor cells. Average body weight of mice was 25−30 g at the time of MRI.

Imaging was performed using a 7 T Varian Unity Inova MRI equipped with a Millipede quadrature RF coil (40 mm ID). A T1-weighted multislice spin echo sequence was performed to record images pre- and postinjection of CAs. The imaging parameters were TE = 15 ms, TR = 500 ms, slice thickness = 1 mm, 17 slices, average = 4, matrix = 128 × 256, and FOV = 35 × 70 mm (coronal). Mice were anesthetized using 2.5% isoflurane in oxygen via a nose cone. Once preinjection imaging had been completed, **CA-12**, **CA-7**, or Omniscan dissolved in 2% Tween-80/PBS was injected through a tail vein (gadolinium dose 0.04 mmol/kg body weight). Mice were imaged immediately after introduction of the CA and again at 30 min, 1 h, 4 h, and 24 h postinjection. A water tube placed under the animal was treated as a reference signal. Vitals were continually monitored, and mice were released to their cage after each imaging session in order to fully recover.

Image analysis and processing were performed with VnmrJ2.1D software (Varian Inc. /Agilent Technologies, 2005). Regions of interest (ROIs) were manually drawn on the tumor tissue, muscle near the tumor, kidney cortex, and liver for each time point. Signal intensity (SI) was measured as the mean of the intensity over the segmented ROIs. SIs were normalized to the SI of muscle with the assumption that signal enhancement of muscle tissue is zero at 4 and 24 h postinjection of CA. The contrast enhancement ratio (CER) for a tissue was calculated according to the equation

$$\mathrm{CER} = (\mathrm{SI}_{\mathrm{post}} - \mathrm{SI}_{\mathrm{pre}})/\mathrm{SI}_{\mathrm{pre}} \times 100\%$$

To assess persistence of the CAs in tissues, mice were euthanized 24 h postinjection. Tumor, blood, heart, lungs, liver, spleen, stomach, large intestine, small intestine, kidney, brain, and muscle samples were collected, weighed, and immediately frozen at −20 °C. Prior to the ICP-OES analysis, tissue samples were allowed to warm up to room temperature and acid digested, and the gadolinium and boron content of the tissues was determined.

Statistical Analysis. Quantitative data were expressed as the mean ± standard deviation (SD). Means were compared by analysis of a student's *t*-test using *t* test function in Microsoft Excel (2007). *P* values of less than 0.05 were considered to be statistically significant.

■ ASSOCIATED CONTENT

Ⓢ Supporting Information

IR spectra, dynamic light scattering, and SE-HPLC analysis data for **CA-7** and **CA-12**. This material is available free of charge via the Internet at http://pubs.acs.org.

■ AUTHOR INFORMATION

Corresponding Author

*E-mail: hawthornem@missouri.edu.

Notes

The authors declare no competing financial interest.

■ ACKNOWLEDGMENTS

This research was funded by National Cancer Institute (Grant R21-CA114090). Authors acknowledge the support provided by the Veterans' Affairs Biomolecular Imaging Center at the Harry S. Truman VA Hospital and the University of Missouri—Columbia. L.M. and Q.C. acknowledge the support from Department of Defense Prostate Cancer Research Program (Grant W81XWH-09-2-0176). We thank Brett Meers, Sarah Higdon, Lisa Watkinson, and Terry Carmack for technical assistance and Pamela Cooper for manuscript editing.

■ REFERENCES

(1) (a) Mansfield, P. *Angew. Chem., Int. Ed.* **2004**, *43*, 5456−5464. (b) Lauffer, R. B. *Chem. Rev.* **1987**, *87*, 901−927. (c) Hermann, P.; Kotek, J.; Kubíček, V.; Lukeš, I. *Dalton Trans.* **2008**, 3027−3047. (d) Caravan, P.; Ellison, J. J.; McMurry, T. J.; Lauffer, R. B. *Chem. Rev.* **1999**, *99*, 2293−2352. (e) Werner, E. J.; Datta, A.; Jocher, C. J.; Raymond, K. N. *Angew. Chem., Int. Ed.* **2008**, *47*, 8568−8580. (f) Caravan, P. *Acc. Chem. Res.* **2009**, *42*, 851−862.

(2) Major, J. L.; Meade, T. J. *Acc. Chem. Res.* **2009**, *42*, 893−899. (b) Caravan, P. *Chem. Soc. Rev.* **2006**, *35*, 512−523.

(3) (a) Park, J.-A.; Lee, J.-J.; Jung, J.-C.; Yu, D.-Y.; Oh, C.; Ha, S.; Kim, T.-J.; Chang, Y. *ChemBioChem* **2008**, *9*, 2811−2813. (b) Verwilst, P.; Eliseeva, S. V.; Carron, S.; Vander Elst, L.; Burtea, C.; Dehaen, G.; Laurent, S.; Binnemans, K.; Muller, R. N.; Parac-Vogt, T. N.; De Borggraeve, W. M. *Eur. J. Inorg. Chem.* **2011**, 3577−3585. (c) Verwilst, P.; Eliseeva, S. V.; Elst, L. V.; Burtea, C.; Laurent, S.; Petoud, S.; Muller, R. N.; Parac-Vogt, T. N.; De Borggraeve, W. M. *Inorg. Chem.* **2012**, *51*, 6405−6411. (d) Dijkgraaf, I.; Rijnders, A. Y.; Soede, A.; Dechesne, A. C.; van-Esse, G. W.; Brouwer, A. J.; Corstens, F. H. M.; Boerman, O. C.; Rijkers, D. T. S.; Liskamp, R. M. J. *Org. Biomol. Chem.* **2007**, *5*, 935−944.

(4) (a) Weinmann, H. J.; Ebert, W.; Misselwitz, B.; Schmitt-Willich, H. *Eur. J. Radiol.* **2003**, *46*, 33−44. (b) Nair, S. A.; Kolodziej, A. F.; Bhole, G.; Greenfield, M. T.; McMurry, T. J.; Caravan, P. *Angew. Chem., Int. Ed.* **2008**, *47*, 4918−4921. (c) Marom, H.; Miller, K.; Bechor-Bar, Y.; Tsarfaty, G.; Satchi-Fainaro, R.; Gozin, M. *J. Med. Chem.* **2010**, *53*, 6316−6325.

(5) (a) Chen, Y. *Theranostics* **2011**, *1*, 28−29. (b) Tan, M.; Lu, Z.-R. *Theranostics* **2011**, *1*, 83−101.

(6) Sipkins, D. A.; Cheresh, D. A.; Kazemi, M. R.; Nevin, L. M.; Bednarski, M. D.; Li, K. C. *Nat. Med.* **1998**, *4*, 623−626.

(7) (a) Mousa, S. A. *Curr. Opin. Chem. Biol.* **2002**, *6*, 534−541. (b) Jin, H.; Varner, J. *Br. J. Cancer* **2004**, *90*, 561−565.

(8) Chen, K.; Chen, Y. *Theranostics* **2011**, *1*, 189−200.

(9) Benedetto, S.; Pulito, R.; Crich, S. G.; Tarone, G.; Aime, S.; Silengo, L.; Hamm, J. *Magn. Reson. Med.* **2006**, *56*, 711−716.

(10) (a) Boswell, C. A.; Eck, P. K.; Regino, C. A. S.; Bernardo, M.; Wong, K. J.; Milenic, D. E.; Choyke, P. L.; Brechbiel, M. W. *Mol. Pharmaceutics* **2008**, *5*, 527−539. (b) De León-Rodríguez, L. M.; Lubag, A.; Udugamasooriya, D. G.; Proneth, B.; Brekken, R. A.; Sun, X.; Kodadek, T.; Sherry, A. D. *J. Am. Chem. Soc.* **2010**, *132*, 12829−12831. (c) Zarabi, B.; Borgman, M. P.; Zhuo, J.; Gullapalli, R.; Ghandehari, H. *Pharm. Res.* **2009**, *26*, 1121−1129. (d) Li, W.; Su, B.; Meng, S.; Ju, L.; Yan, L.; Ding, Y.; Song, Y.; Zhou, W.; Li, H.; Tang, L.; Zhao, Y.; Zhou, C. *Eur. J. Radiol.* **2011**, *80*, 598−606.

(11) (a) Bryson, J. M.; Chu, W.; Lee, J.; Reineke, T. M. *Bioconjugate Chem.* **2008**, *19*, 1505−1509. (b) Song, Y.; Kohlmeir, E. K.; Meade, T. J. *J. Am. Chem. Soc.* **2008**, *130*, 6662−6663. (c) Livramento, J. B.; Helm, L.; Sour, A.; O'Neil, C.; Merbach, A. E.; Tóth, É. *Dalton Trans.* **2008**, 1195−1202. (d) Langereis, S.; de Lussanet, Q. G.; van Genderen, M. H. P.; Backes, W. H.; Meijer, E. W. *Macromolecules* **2004**, *37*, 3084−3091. (e) Torchilin, V.; Babich, J.; Weissig, V. *J. Liposome Res.* **2000**, *10*, 483−499. (f) Kielar, F.; Tei, L.; Terreno, E.; Botta, M. *J. Am. Chem. Soc.* **2010**, *132*, 7836−7837. (g) Floyd, W. C.; Klemm, P. J.; Smiles, D. E.; Kohlgruber, A. C.; Pierre, V. C.; Mynar, J.

L.; Fréchet, J. M. J.; Raymond, K. N. *J. Am. Chem. Soc.* **2011**, *133*, 2390−2393.
(12) (a) Hawthorne, M. F.; Maderna, A. *Chem. Rev.* **1999**, *99*, 3421−3434. (b) Hawthorne, M. F.; Farha, O. K.; Julius, R.; Ma, L.; Jalisatgi, S. S.; Li, T.; Bayer, M. J. *ACS Symp. Ser.* **2006**, *917*, 312−324. (c) Issa, F.; Kassiou, M.; Rendina, L. M. *Chem. Rev.* **2011**, *111*, 5701−5722.
(13) Bayer, M. J.; Hawthorne, M. F. *Inorg. Chem.* **2004**, *43*, 2018−2020.
(14) (a) Jalisatgi, S. S.; Kulkarni, V. S.; Tang, B.; Houston, Z. H.; Lee, M. W.; Hawthorne, M. F. *J. Am. Chem. Soc.* **2011**, *133*, 12382−12385. (b) Goswami, L. N.; Chakravarty, S.; Lee, M. W.; Jalisatgi, S. S.; Hawthorne, M. F. *Angew. Chem., Int. Ed.* **2011**, *50*, 4689−4691.
(15) Goswami, L. N.; Ma, L.; Chakravarty, S.; Cai, Q.; Jalisatgi, S. S.; Hawthorne, M. F. *Inorg. Chem.* **2013**, DOI: 10.1021/ic3017613 (Article ASAP).
(16) Goswami, L. N.; Houston, Z. H.; Sarma, S. J.; Li, H.; Jalisatgi, S. S.; Hawthorne, M. F. *J. Org. Chem.* **2012**, *77*, 11333−11338.
(17) Barge, A.; Cravotto, G.; Gianolio, E.; Fedeli, F. *Contrast Media Mol. Imaging* **2006**, *1*, 184−188.
(18) Goswami, L. N.; Houston, Z. H.; Sarma, S. J.; Jalisatgi, S. S.; Hawthorne, M. F. *Org. Biomol. Chem.* **2013**, *11*, 1116−1126.
(19) Takayama, S.; Ishii, S.; Ikeda, T.; Masamura, S.; Doi, M.; Kitajima, M. *Anticancer Res.* **2005**, *25*, 79−84.